BINARY-VALUED WAVELET DECOMPOSITIONS OF BINARY IMAGES *

Mitchell D. Swanson and *Ahmed H. Tewfik*
Department of Electrical Engineering, University of Minnesota
Minneapolis, MN 55455
e-mail: {*mswanson,tewfik*}*@ee.umn.edu*

ABSTRACT

We introduce a binary-valued wavelet decomposition of binary images. Based on simple modulo-2 operations, the transform is computationally simple and immune to quantization effects. The new transform behaves like its real-valued counterpart. In particular, it yields an output similar to the thresholded output of a real wavelet transform operating on the underlying binary image. Using a new binary field transform to characterize binary filters, binary wavelets are constructed in terms of 2-band perfect reconstruction filter banks. We include lossless image coding results to illustrate the compactness of the representation.

1 INTRODUCTION

The development of wavelet theory has occurred mostly for real-valued signals. In particular, the data to be analyzed, the families of basis functions, and the transform coefficients are all real-valued. In this paper, we present a *binary-valued* wavelet decomposition of binary (i.e., $GF(2)$) images. The binary wavelet transform that we construct shares many of the important characteristics of the real wavelet transform. In particular, it yields an output that is similar to a thresholded real field wavelet transform of the underlying binary image (c.f. Figs. 3 and 4). Therefore, our binary wavelet transform of binary images can be used as a *fast and lossless alternative* to the real-valued wavelet transform of these images in binary image processing applications (e.g., coding, edge detection, recognition, etc.).

The binary wavelet transform has several distinct advantages over the real transform when applied to thresholded or binary (e.g., fingerprints, facsimiles) data. First, all data produced by the binary wavelet transform are binary. No quantization effects are introduced. Second, as modulo-2 arithmetic is equivalent to exclusive-OR operations, the transform is very fast. Finally, as the data remains binary, operations on the transformed data tend to be much simpler.

*This work was supported by ARPA under grant AF/F49620-93-10528 administered by AFOSR and partially by AFOSR under grant AF/49620-93-0151DEF.

Extensions of wavelet theory to finite fields have been investigated. The difficulties associated with the design of filter banks in $GF(2)$ are discussed in [1]. Others have extended wavelet theory to finite fields with characteristics other than 2 (e.g., [2]). In this paper, we extend our previous results [3]. We construct wavelet decompositions in $GF(2)$ by introducing a new binary field transform which characterizes the filtering properties (e.g., lowpass, highpass, etc.) of binary signals. The new transform allows us to avoid Fourier transform techniques which are limited over $GF(2)$. Using the new transform, we construct binary wavelets based on 2-band perfect reconstruction filter banks in $GF(2)$. The work presented here modifies of our previous binary field transform [3], explains filter design, and includes experimental coding results.

2 $GF(2)$ ALGEBRA AND NOTATION

While certain properties of matrices over the binary field differ from properties of matrices over the real field, matrix arithmetic (i.e., multiplication, inversion, etc.) is performed the same in $GF(2)$. The only difference is that all computations are followed by a modulo-2 operation. We denote by $A(j,k)$ the (j,k) element of matrix $\mathbf{A}$, and by $v(k)$ the k element of vector $\mathbf{v}$. $\mathbf{A}(:,j)$ and $\mathbf{A}(i,:)$ are the j^{th} column and i^{th} row of $\mathbf{A}$, respectively. All indices start at 0.

In addition, we denote by $1-circ(\mathbf{v})$ a *one*-circulant matrix whose rows are generated by successive shifts by one of the first row $\mathbf{v}$ in the matrix. We also consider *two*-circulant matrices $2-circ(\mathbf{v})$ which have the form

$$\mathbf{L} = \begin{bmatrix} v_0 & v_1 & v_2 & \dots & v_{N-1} \\ v_{N-2} & v_{N-1} & v_0 & \dots & v_{N-3} \\ v_{N-4} & v_{N-3} & v_{N-2} & \dots & v_{N-5} \\ \vdots & \vdots & \vdots & \ddots & \vdots \\ v_2 & v_3 & v_4 & \dots & v_1 \end{bmatrix}. \quad (1)$$

3 BINARY FIELD TRANSFORM

The Fourier transform is usually used to characterize real-valued filters. Unfortunately, the Fourier transform of sequences over $GF(2)$ is only defined for sequences of length 1 [4]. To avoid the complexity of introducing

extension fields, we introduce *a new binary field transform* (BFT) to characterize filtering properties of binary signals. Our original BFT [3] has been modified here to facilitate binary filter design.

Instead of the traditional sine and cosine basis functions, the basis functions of the BFT are rectangular waveforms which take on values 1 and 0 with a certain *sequency*. We define the sequency of a binary waveform as the number of transitions, k, from '0' to '1' and '1' to '0' per period divided by two for k even ($(k+1)/2$ for k odd). These basis functions constitute the columns of our BFT matrices.

The $N \times N$ BFT matrices $\mathbf{B}_N$ are defined recursively. We define

$$\mathbf{B}_2 = \begin{bmatrix} 1 & 1 \\ 1 & 0 \end{bmatrix}, \quad \text{and} \quad \mathbf{B}_4 = \begin{bmatrix} 1 & 1 & 1 & 1 \\ 1 & 1 & 0 & 0 \\ 1 & 0 & 1 & 1 \\ 1 & 0 & 1 & 0 \end{bmatrix}.$$

For $N \geq 6$ and even, we construct $\mathbf{B}_N$ in terms of four submatrices as

$$\mathbf{B}_N = \begin{bmatrix} \mathbf{B}_N^{ul} & \mathbf{B}_N^{ur} \\ \mathbf{B}_N^{ll} & \mathbf{B}_N^{lr} \end{bmatrix}. \tag{2}$$

The upper-left $(N-2) \times (N-2)$ submatrix $\mathbf{B}_N^{ul}$, the upper-right $(N-2) \times 2$ submatrix $\mathbf{B}_N^{ur}$ $(= \mathbf{B}_N^{llT})$, and lower-right 2×2 submatrix $\mathbf{B}_N^{lr}$ are defined as

$$\mathbf{B}_N^{ul} = \begin{bmatrix} \mathbf{1s}_{2\times 2} & \mathbf{1s}_{2\times(N-4)} \\ \mathbf{1s}_{(N-4)\times 2} & \overline{\mathbf{B}}_{(N-4)} \end{bmatrix},$$

$$\mathbf{B}_N^{ur} = \mathbf{B}_N^{llT} = \begin{bmatrix} 1 & 1 \\ 0 & 0 \\ 1 & 1 \\ 0 & 0 \\ \vdots & \vdots \end{bmatrix}, \quad \text{and} \quad \mathbf{B}_N^{lr} = \begin{bmatrix} 1 & 1 \\ 1 & 0 \end{bmatrix}.$$

The matrix $\mathbf{1s}_{N\times M}$ is an $N \times M$ matrix that consists of 1's. Matrix $\overline{\mathbf{B}}_{N-4}$ is the result of applying the logical-NOT operation to each element of the BFT matrix $\mathbf{B}_{N-4}$. For N odd, we construct $\mathbf{B}_{N+1}$ and define $\mathbf{B}_N$ as the upper-left $N \times N$ submatrix $\mathbf{B}(0:N-1, 0:N-1)$ of $\mathbf{B}_{N+1}$.

By construction, each $\mathbf{B}_N$ is invertible over $GF(2)$ and a closed form formula provides the inverse $\mathbf{B}_N^{-1}$ of $\mathbf{B}_N$ [6]. Note that our BFT matrices take an analogous form to sequency ordered Walsh-Hadamard transform matrices [5]. In particular, the sequency ordering of the columns corresponds to a nondecreasing sequency ordering of Walsh functions. As an example, consider the 8×8 BFT matrix (from left to right, the sequency value of each column is 0, 1, 1, 2, 2, 3, 3, 4)

$$\mathbf{B}_8 = \begin{bmatrix} 1 & 1 & 1 & 1 & 1 & 1 & 1 & 1 \\ 1 & 1 & 1 & 1 & 1 & 1 & 0 & 0 \\ 1 & 1 & 0 & 0 & 0 & 0 & 1 & 1 \\ 1 & 1 & 0 & 0 & 1 & 1 & 0 & 0 \\ 1 & 1 & 0 & 1 & 0 & 0 & 1 & 1 \\ 1 & 1 & 0 & 1 & 0 & 1 & 0 & 0 \\ 1 & 0 & 1 & 0 & 1 & 0 & 1 & 1 \\ 1 & 0 & 1 & 0 & 1 & 0 & 1 & 0 \end{bmatrix}.$$

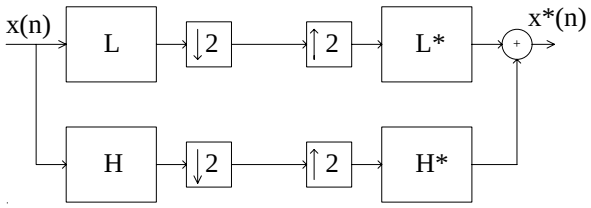

Figure 1: 2-band perfect reconstruction filter bank.

4 BINARY FILTER CHARACTERIZATION

Using the BFT, we replace conventional Fourier frequency information with sequency information. However, the BFT of a sequence is computed in a manner that is different from that commonly associated with the DFT. Rather than computing the matrix-vector product $\mathbf{B}_N^{-1}\mathbf{x}$ for a length N sequence $\mathbf{x}$, we apply $\mathbf{B}_N^{-1}$ to all circular shifts of $\mathbf{x}$. Specifically, to compute the $N \times N$ matrix BFT $\hat{\mathbf{X}}$ of $\mathbf{x}$, we begin by forming the equivalent *one*-circulant matrix $\mathbf{X} = 1 - circ(\mathbf{x})$. We then evaluate the matrix-matrix product $\hat{\mathbf{X}} = \mathbf{X}\mathbf{B}_N^{-1}$. This definition of spectrum in $GF(2)$ is motivated by the fact that a circular shift of $\mathbf{x}$ can lead to a different transform. In particular, a shift by one unit in the discrete time domain is not equivalent to multiplication of the transform by a simple factor as with the Fourier transform on the real field. Another advantage of this definition is that it allows us to *define the magnitude of the spectral components of* $\mathbf{x}$ *along each BFT basis vector simply by counting the number of 1's in the corresponding column of* $\hat{\mathbf{X}}$.

A limitation of the BFT, as defined above, is that the circular convolution of two sequences is *not* equivalent to multiplication of their transforms in the BFT domain. In particular, a filter that has large spectral components at high sequencies need not be a high pass filter! To characterize a filter as lowpass, highpass, etc., we need to examine its effect on the *basis vectors* of a BFT. This is done by evaluating the circular convolution of the filter with each basis vector via the product $\tilde{\mathbf{X}} = \mathbf{X}\mathbf{B}_N$. Note that this is akin to evaluating a BFT with respect to the *inverse* BFT matrix $\mathbf{B}_N^{-1}$. We refer to $\tilde{\mathbf{X}}$ as the *filter* BFT (FBFT) of $\mathbf{x}$.

5 BINARY WAVELETS

We view the design of 2-band discrete orthonormal binary wavelets as equivalent to the design of a 2-band perfect reconstruction (PR) filter bank with added regularity conditions. The 2-band PR filter bank is shown in Fig. 1, where the input signal is simultaneously passed through lowpass L (scaling coefficients $\mathbf{l}$) and highpass H (wavelet coefficients $\mathbf{h}$) filters and then decimated by 2 to give us approximation and detail components of the original signal. The two decimated signals may then be upsampled and passed through complementary filters and summed to reconstruct our original signal.

To ensure that we can perform a useful multiresolution decomposition and still be able to reconstruct our original signal, the filters must satisfy 3 constraints: bandwidth, vanishing moments, and perfect reconstruction. A modified version of the FBFT of the previous section is used to characterize the filters L and H. Specifically, since we subsample the outputs of the lowpass and highpass filters by 2, we take into account decimation operation by first forming the equivalent *two*-circulant matrices (Eq. 1) $\mathbf{L}_2 = 2 - circ(\mathbf{l})$ and $\mathbf{H}_2 = 2 - circ(\mathbf{h})$. Next, we compute the size $N/2 \times N$ decimated FBFT's $\tilde{\mathbf{L}}_2$ and $\tilde{\mathbf{H}}_2$ by retaining every other row of $\tilde{\mathbf{L}}$ and $\tilde{\mathbf{H}}$ respectively, i.e.,

$$\begin{array}{c} \tilde{\mathbf{L}}_2 = \mathbf{L}_2\mathbf{B}_N = \tilde{\mathbf{L}}(0:2:N-1,:) \\ \tilde{\mathbf{H}}_2 = \mathbf{H}_2\mathbf{B}_N = \tilde{\mathbf{H}}(0:2:N-1,:). \end{array} \tag{3}$$

For the bandwidth condition, we restrict the bandwidths of $\mathbf{l}$ and $\mathbf{h}$ to be approximately equal in size, i.e., the number of nonzero columns of $\tilde{\mathbf{L}}_2$ and $\tilde{\mathbf{H}}_2$ are approximately equal. This helps maintain an even distribution of sequency content in the filter outputs. In addition, we require $\mathbf{l}$ to be a lowpass filter, i.e., we set $\tilde{\mathbf{L}}_2(:, N-1) = \mathbf{0}_{N/2\times 1}$.

The vanishing moments property of wavelets over the real field ensures that the Fourier transform of the wavelet coefficients will have zeros of a certain order at DC, i.e., it will decay smoothly to zero as the frequency approaches zero. In particular, a large number of vanishing moments leaves minimal power in the low frequency region of the Fourier transform of the wavelet which results in a *better low frequency attenuation* performance.

The vanishing moments constraint that real wavelet filters satisfy is replaced by a constraint in $GF(2)$ on the number of low and high sequency basis vectors that the highpass and lowpass filter block respectively. As we cannot have a "smooth" decay to zero in $GF(2)$, the frequency domain smooth decay to zero as frequency approaches zero and high attenuation characteristics at low frequencies are replaced with multiple consecutive zeros at low sequency in the FBFT matrix. This property allows for a more compact representation of slowly varying $GF(2)$ sequences (c.f. Sect. 6). Compactness means here that filtered sequences consist mostly of zeros. The additional zeros at low sequency allow us to avoid representing (passing) the slowly varying regions in an input sequence.

In terms of the FBFT, $\tilde{\mathbf{H}}_2(:,0) = \mathbf{0}_{N/2\times 1}$. This equation guarantees one vanishing moment. We can maximize the number of vanishing moments by forcing the filter $\mathbf{h}$ to block the first $N/2$ low sequency basis components, i.e., $\tilde{\mathbf{H}}_2(:,i) = \mathbf{0}$ for $i = 0, \ldots, N/2-1$. As in the real case, the resulting wavelet filter would then have a better highpass characteristic. Note that, similar to the real case, we can set no more than $N/2$ columns of the FBFT matrix corresponding to the highpass filter equal to zero. If we try to do so, we end up with an overdetermined and inconsistent set of equations.

Finally, we impose the perfect reconstruction constraint to guarantee that the binary wavelet transform is invertible. Using the *two*-circulant matrices $\mathbf{L}_2$ and $\mathbf{H}_2$ of the filter coefficients, we can compute the operation of the filter bank by applying the matrix

$$\mathbf{T} = \begin{bmatrix} \mathbf{L}_2 \\ \mathbf{H}_2 \end{bmatrix}$$

to the length N input data sequence. Perfect reconstruction is guaranteed if the matrix $\mathbf{T}$ is invertible. In [6], we show that $\mathbf{T}$ is invertible if and only if the filter coefficients l_i and h_i satisfy

$$\det(\mathbf{T}) = \sum_{i=0,even}^{N-2} l_i \sum_{i=1,odd}^{N-1} h_i + \sum_{i=1,odd}^{N-1} l_i \sum_{i=0,even}^{N-2} h_i = 1.$$

Now observe that the lowpass condition on $\mathbf{l}$ and single vanishing moment condition on $\mathbf{h}$ imply

$$\sum_{i=0,even}^{N-2} l_i = \sum_{i=0}^{N-1} h_i = 0. \tag{4}$$

Therefore, we conclude that we must also have

$$\sum_{i=1,odd}^{N-1} l_i = \sum_{i=0,even}^{N-2} h_i = \sum_{i=1,odd}^{N-1} h_i = 1. \tag{5}$$

The above equations are also equivalent to $\tilde{\mathbf{L}}_2(:,0) = \tilde{\mathbf{H}}_2(:,N-1) = \mathbf{1}_{N/2\times 1}$

6 EXAMPLES

We design a wavelet with 2 vanishing moments using the theory described above. First, we restrict the wavelet filter coefficients $\mathbf{h}$ using Eq. 5 which requires $h_0 + h_2 = h_1 + h_3 = 1$. This guarantees PR and one vanishing moment for $\mathbf{h}$. The second vanishing moment requires (second column of $\tilde{\mathbf{H}}_2 = \mathbf{H}_2\mathbf{B}_N$) $h_0 + h_1 = h_2 + h_3 = 0$. By combining these two sets of equations, we find that $\mathbf{h} = [h_0 \; h_0 \; (1+h_0) \; (1+h_0)]$. Since $h_0 = 0$ or 1, we have two possible wavelet filters with 2 vanishing moments: [1 1 0 0] or [0 0 1 1]. The lowpass filter is designed similarly by blocking high sequency BFT basis vectors.

Defining 2D filters as tensor products of $\mathbf{h} = [1\,1\,0\,0]$ and $\mathbf{l} = [1\,1\,1\,0]$, we performed a 3-stage decomposition of the 256×256 binary ship image shown in Fig. 2. The result is shown in Fig. 3. The upper-left and lower-right subbands correspond to low sequency and high sequency components, respectively. Note that the higher sequency edge transitions mapped into higher sequency subbands. Of the original 65536 pixels, the original image has 35414 nonzero pixels, while the transform has only 2199 nonzero pixels. Using an entropy-based cost function $H(p) = -p\log_2(p) - (1-p)\log_2(1-p)$, where where p is the number of nonzero pixels in the image divided by the total number of pixels in the image, this corresponds to a decrease in entropy from 0.995 bpp

to 0.212 bpp. A small value for H indicates a large discrepancy between the number of zero and nonzero coefficients and a more efficient coding representation. A real-valued Daubechies wavelet transform with two vanishing moments was also applied to the image. The result of applying a threshold operator to the real-valued wavelet decomposition is shown in Fig. 4. Coefficients > 0 are shown in white. The results are almost identical.

We also coded several binary images and their corresponding binary wavelet transform subbands using a run-length coder. The 256×256 binary test images included letters (e.g., 'a', 'b', etc.) and facsimiles of typed and handwritten data. Our results, shown in Table 1, indicate that entropy was significantly reduced in the transformed images. In addition, run-length results indicate savings in storage requirements ranging from 25% to over 100% over similarly coded original images.

Table 1: Summary of Coding Results for Letters and Facsimiles. Originals: 256x256=8192 Bytes. H: entropy. R-L: run-length (Bytes).

Image	Orig. H	Trans. H	Orig. R-L	Trans. R-L	Gain (%)
'a'	0.706	0.158	320	220	45.5
'b'	0.753	0.168	315	182	73.1
'c'	0.596	0.128	257	186	38.2
'd'	0.765	0.174	353	218	61.9
'e'	0.630	0.137	261	195	33.9
FAX1	0.331	0.249	1035	794	30.4
FAX2	0.261	0.240	1375	571	140.8
FAX3	0.489	0.266	1213	733	65.5
FAX4	0.617	0.269	1238	995	24.4
FAX5	0.439	0.248	1146	914	25.4
FAX6	0.395	0.251	1369	860	59.2

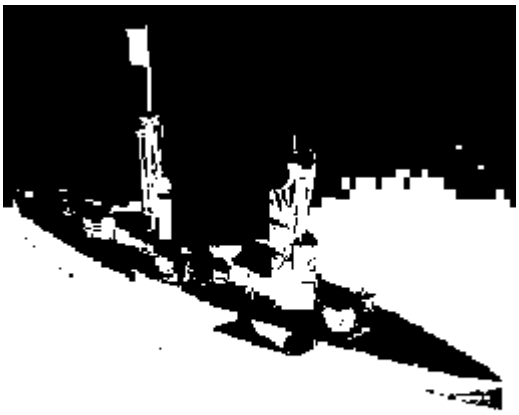

Figure 2: Original binary ship image (256x256).

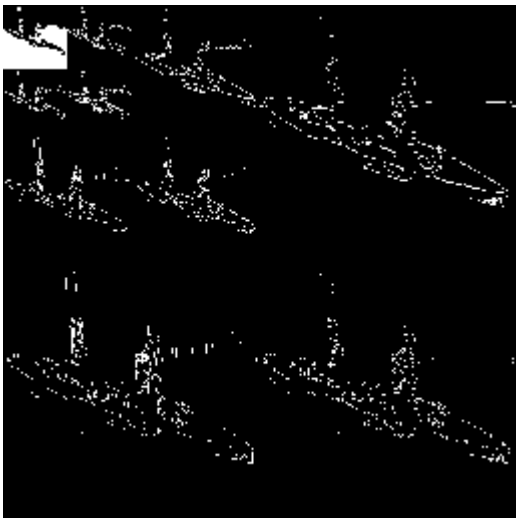

Figure 3: 3-stage binary wavelet transform of ship.

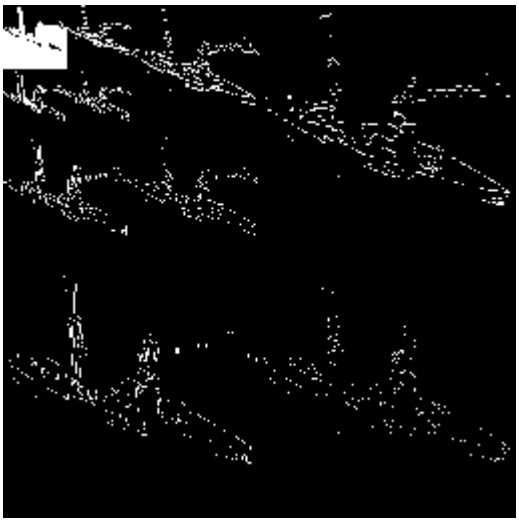

Figure 4: 3-stage thresholded real wavelet transform of ship.

References

[1] S. M. Phoong and P. P. Vaidyanathan, "Paraunitary Filter Banks over Finite Fields," preprint, Oct. 1995.

[2] G. Caire, R. L. Grossman, and H. V. Poor, "Wavelet Transforms Associated with Finite Cyclic Groups," *IEEE Trans. on Info. Theory*, vol. 39, pp. 1157–1166, July 1993.

[3] M. D. Swanson and A. H. Tewfik, "Wavelet Decomposition of Binary Finite Images," in *Proc. IEEE Int. Conf. on Image Proc.*, Austin, TX, vol. I, pp. 61–65, 1994.

[4] R. E. Blahut, *Algebraic Methods for Signal Processing and Communications Coding.* New York: Springer-Verlag, Inc., 1992.

[5] N. Ahmed and K. R. Rao, *Orthogonal Transforms for Digital Signal Processing.* New York: Springer-Verlag, Inc., 1975.

[6] M. D. Swanson and A. H. Tewfik, "A Binary Wavelet Decomposition of Binary Images," *IEEE Trans. on Image Proc.*, to appear Nov., 1996. Available *http://www.ee.umn.edu/groups/msp.*